

MOL #68767

**Glycine hinges with opposing actions at the acetylcholine receptor-channel
transmitter binding site**

Prasad Purohit and Anthony Auerbach

Department of Physiology and Biophysics, SUNY at Buffalo, Buffalo 14214, USA

MOL #68767

a) Running title: AChR transmitter binding site

b) Corresponding author:

Anthony Auerbach,

email: auerbach@buffalo.edu

309C Cary Hall, South Campus, SUNY at Buffalo

Buffalo NY 14214

Phone 716-829-3450

Fax 716-829-2569

c) 1. number of text pages: main manuscript 36, Supplementary data: 11

2. number of tables: main manuscript 01, Supplementary data: 05

3. number of figures: main manuscript 05, Supplementary data: 04

4. number of references: main manuscript 42, Supplementary data: 06

5. number of words in the Abstract: 141,

6. number of words in the Introduction: 615

7. number of words in the Discussion: 1626

d) Non-standard abbreviations:

nicotinic acetylcholine receptor, AChR; wild-type, wt; acetylcholine, ACh; choline, Cho; resting-closed AChRs, R; active-open state AChRs, R*; diliganded/unliganded gating equilibrium constant, E_2/E_0 ; forward/backward gating rate constants f_2/b_2 ; single-site association/dissociation rate constant, k_+/k_- ; resting/active state equilibrium dissociation constant, K_d/J_d ; the agonist affinity ratio, λ .

MOL #68767

Abstract

The extent to which agonists activate synaptic receptor-channels depends on both the intrinsic tendency of the unliganded receptor to open and the amount of agonist binding energy realized in the channel-opening process. We examined mutations of the nicotinic acetylcholine receptor transmitter binding site (α subunit loop B) with regard to both of these parameters. α G147 is an 'activation' hinge where backbone flexibility maintains high values for intrinsic gating, the affinity of the resting conformation for agonists and net ligand binding energy. α G153 is a 'deactivation' hinge that maintains low values for these parameters. α W149 (between these two glycines) mainly serves to provide ligand binding energy for gating. We propose that a concerted motion of the two glycine hinges (plus other structural elements at the binding site) positions α W149 so that it provides physiologically-optimal binding and gating function at the nerve-muscle synapse.

MOL #68767

Introduction

At the vertebrate neuromuscular synapse, transmitter molecules released from the nerve terminal bind at two specific sites in the extracellular domain of the nicotinic acetylcholine receptor (AChR) to promote opening of a distant ion channel and depolarization of the muscle cell membrane (Auerbach, 2010; Edelstein and Changeux, 1998; Karlin, 2002). The equilibrium constant of the AChR ‘gating’ conformational change is coupled to an affinity change for agonists at the transmitter binding sites. Acetylcholine (ACh) binds more tightly to active-open (R^*) compared to resting-closed (R) AChRs, hence liganded receptors adopt the R^* , open-channel conformation with a higher probability than do unliganded ones. Each AChR transmitter binding site is comprised, in part, of three loops in the α subunit. Here we are concerned with the roles of residues in loop B with regard to the agonist affinity change and the global gating isomerization.

The probability of adopting R^* is reduced by mutations of aromatic residues at the binding sites (Abramson et al., 1989; Akk, 2001; Aylwin and White, 1994; Chen et al., 1995; Chiara et al., 1998; Cohen et al., 1991; Dennis et al., 1988; Galzi et al., 1990; Middleton and Cohen, 1991; O’Leary et al., 1994; Sine et al., 1994). The mutations of α W149 (loop B) and α Y190 (loop C) decrease the affinity of the R conformation for ACh but, to an even greater extent, that of the R^* conformation (Purohit and Auerbach, 2010). Residues α Y93 (loop A), α Y198 (loop C) and ϵ/δ subunit position W55/W57 (loop D) show similar, but less pronounced, behaviors. Most of these mutations have relatively smaller effects on the unliganded gating equilibrium constant (E_0), so the primary mechanism by which they decrease activation of fully-liganded AChRs is by

MOL #68767

decreasing the net ligand binding energy available for gating. This energy is proportional to the natural logarithm of the R/R* equilibrium dissociation constant ratio (λ , the ‘coupling’ constant). Loop B contains two glycines at positions α G147 and α G153 and a conserved Trp at position α W149. Our goal was to estimate the effects of mutations of these and other loop B amino acids with regard to both E_0 and λ .

Some loop B residues have been studied previously. α G153S is a slow channel congenital myasthenic mutation (Sine et al., 1995) that yields AChRs with a higher R-conformation affinity for the transmitter and an increased intrinsic gating isomerization constant (Zhou et al., 1999). This residue has recently been suggested to be important with regard to setting the AChR affinity specifically for the partial agonist nicotine (Xiu et al., 2009). α W149 has long been known to play a central role in both agonist binding and channel gating (Akk, 2001; Zhong et al., 1998). Many mutations here increase E_0 (Purohit and Auerbach, 2010), but, because they also substantially reduce the R affinity, their effects on liganded gating have not yet been quantified. Less is known about the contributions of other loop B residues in ligand binding and channel gating. α T148 and α T150 mutations have little effect on agonist binding or channel gating (Cashin et al., 2007; Lee and Sine, 2004), α Y151 is required for strong binding of imidacloprid to insect AChRs (Liu et al., 2005), and α D152 is important for setting both the affinity of the resting binding site and the diliganded gating equilibrium constant (Sugiyama et al., 1996; Zhou, 1999). In sum, pieces of information about ligand binding and channel gating are known for loop B residues, but a full exposition of the effects of mutations here is currently not available.

MOL #68767

We have carried out a systematic single-channel study of α subunit loop B residues, α G147- α G153. For each position we dissect the underlying cause of its influence on AChR function with regard to E_0 and λ .

MOL #68767

Materials and Methods

Mutagenesis and expression

Mutants were made by using the QuikChange site-directed mutagenesis kit (Stratagene) and were confirmed by complete cDNA sequencing. Human embryonic kidney cells (HEK293) were transiently transfected using calcium-phosphate precipitation with a mixture of cDNAs encoding mouse muscle AChRs (α , β , δ and ϵ ; ~3-4 $\mu\text{g}/35$ mm dish, in the ratio 2:1:1:1). cDNA (0.1 $\mu\text{g}/\mu\text{l}$) encoding green fluorescent protein was added as a marker to the transfection cocktail. The cells were incubated at 37°C, the culture medium was washed after ~16 h and single-channel patch clamp recording was performed in the cell-attached configuration ~4-6 h later at 23 °C. The bath solution was usually Dulbecco's phosphate buffered saline (PBS) containing (in mM): 137 NaCl, 0.9 CaCl₂, 2.7 KCl, 1.5 KH₂PO₄, 0.5 MgCl₂, and 8.1 Na₂HPO₄ (pH 7.4). Sometimes in the bath solution NaCl was replaced with KCl (K-PBS). The pipette solution was always PBS. In some experiments an agonist (acetylcholine or choline) was added only to the pipette solution. The pipette potential was either +70 (PBS) or -70 mV (K-PBS), which corresponds to membrane potentials of approximately -100 or exactly +70 mV. Currents were sampled at 50 kHz after low-pass filtering at 20 kHz. QuB software (qub.buffalo.edu) was used to acquire and analyze the single-channel currents.

The single-channel currents were corrected for baseline drift. Clusters of single-channel openings, that each reflect binding and gating events of an individual AChR, were selected by eye and idealized into noise-free conducting/non-conducting intervals by using the segmental-k-means algorithm (Qin, 2004). To estimate the gating rate constants, the idealized current interval durations were modeled (see below) using a maximum interval

MOL #68767

likelihood method after imposing a 25 μ s dead time and approximate missed-event correction (Qin et al., 1997).

The scheme we used for interpreting the functional properties of AChRs is shown in Fig 1B. The diliganded gating equilibrium constant (E_2) was calculated as the ratio of the forward/backward isomerization rate constants (f_2/b_2). Choline was used to activate constructs in which E_2 was approximately equal to or larger than the wild-type (wt) and ACh was used to activate constructs in which E_2 was smaller than the wt. In most experiments, the initial test agonist concentration was either 20 mM choline or 1 mM ACh.

Some loop B mutations caused a severe loss of activity so that openings were not clustered even at these high agonist concentrations. To compensate, we co-expressed these mutants with an ϵ subunit having two transmembrane domain background mutations, ϵ (P245L+L269F). Together, these two mutations increase f_2 by ~14-fold and decrease b_2 by ~33-fold (increase E_2 by ~450-fold). The background mutations were located far from loop B we assumed that their effects and those at loop B were energetically independent.

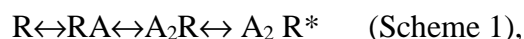
In some experiments we fully-saturated the transmitter binding sites by using 140 mM acetylcholine, a concentration that is ~1000 times larger than the resting equilibrium dissociation constant (K_d) of wt AChRs (Chakrapani et al., 2003). To be sure that this concentration fully saturated the binding sites, we also measured the gating rate constants at 100 mM ACh. If the effective opening rate was approximately the same at both concentrations we considered the binding sites to be completely saturated (Fig. S2).

At these high ACh concentrations open-channel block by the agonist reduced the current amplitude almost to zero. To compensate, in some experiments the pipette was held at -70 mV (which corresponds to a membrane potential of +70 mV) and the kinetic

MOL #68767

parameters of the outward, single-channel currents were quantified. Depolarization also changes the gating rate constants. Because we wanted to compare the measured equilibrium and rate constants to wt values obtained at a physiological membrane voltage (~-100 mV) we used correction factors that pertain to a 170 mV depolarization, which alone causes a 1.5-fold decrease in f_2 and 10-fold increase in b_2 (a 15-fold decrease in E_2) (Auerbach et al., 1996; Jha et al., 2009). We assumed that the voltage and mutation perturbations are energetically independent. The background perturbation corrected constants are reported in Table S1. All experiments with 20 mM choline were at -100 mV membrane potential. To correct for the effect of channel-block on b_2 we multiplied the observed value by 3.1 (corrected values shown in Table S1) (Jha et al., 2009).

K_d was estimated for some mutants (Fig. 3, Table S4). For the α G153 series, AChRs were activated by using three different choline concentrations and interval durations within clusters were fitted together by using the following kinetic scheme,



where A is the agonist. We assumed that the two binding steps are equal and independent (Akk et al., 1996; Jha et al., 2009; Salamone et al., 1999) so only four rate constants were free parameters: single-site association (k_+) scaled by the agonist concentration, single-site dissociation (k_-), f_2 and b_2 . K_d was calculated as the ratio k_-/k_+ . For α G147S the relationship between the [ACh] and the open probability of clusters (P_o) was fitted by (from Scheme 1):

$$P_o = (c^2 E_2) / (1 + 2c + c^2 + c^2 E_2)$$

$$c = [\text{ACh}] / K_d.$$

At each ACh concentration P_o was calculated from the rate constants, $P_o = f_2 / (f_2 + b_2)$.

MOL #68767

In wild type (wt) AChRs unliganded (spontaneous) openings are both rare and brief. To increase both the frequency and duration of such openings we used a background construct that had multiple point mutations in both α subunits (α D97A+ α Y127F+ α S269I; 'DYS'). Individually, each of these mutations increases the diliganded gating equilibrium constant [α D97A, 168-fold (Chakrapani et al., 2003); α Y127F, 59-fold (Purohit and Auerbach, 2007); α S269I, 115-fold (Mitra et al., 2005)] by an approximately parallel change in the unliganded gating equilibrium constant (Purohit and Auerbach, 2009). None of these mutations has a significant effect on K_d . The fold-changes in E_0 for the loop B mutations in this study are expressed in reference to the DYS background, so the only assumption we make is that the loop B and DYS mutations have independent energetic consequences. There was no agonist-associated open-channel block in experiments without agonists in the pipette solution and the single-channel current amplitude was in all cases ~ 7 pA at a pipette potential of +70 mV.

For some mutants the spontaneous open- and closed-interval durations within clusters were well described by a single exponential component. For these, f_0 and b_0 were simply the inverse mean lifetimes of the non-conducting and conducting intervals. In some constructs there were multiple open/shut components, and for these the intracluster interval durations were fitted by using a kinetic model having two non-conducting and two conducting states. We tested both coupled and uncoupled kinetic schemes, with nearly equivalent results for the E_0 estimate. The values reported in the Tables were obtained by using a coupled conducting-state model (CCOO), with E_0 calculated as the ratio of f_0/b_0 associated with the predominant (typically, $\sim 90\%$), brief open component.

MOL #68767

For each mutant, the fold-change in parameter X was estimated as $(X^{\text{mutant}}/X^{\text{background}})$. The change in the free energy ($\Delta\Delta G$, in kcal/mol) caused by mutation was calculated as $-0.59\ln(\text{fold-change})$. The coupling energy between side-chains was calculated as $-0.59\ln(X^{\text{observed}}/X^{\text{predicted}})$, where the predicted value was calculated as the sum of the $\Delta\Delta G$ values for each individual mutation.

For all constructs, example currents are shown in Fig. S1 and the rate constants are shown in Tables S1 and S2. Below, the kinetic parameters are displayed in the form of rate-equilibrium (R/E) relationships, in which the forward isomerization rate constant is plotted as a function of the gating equilibrium constant for a family of mutations of that residue on a log-log scale (Fersht, 1995). The ‘range-energy’ is the natural logarithm of the ratio of the largest/smallest equilibrium constant for a series of mutations of one position (Jha et al., 2009). Φ is the linear slope of the R/E relationship and provides information about the relative timing of the energy change of the perturbed residue, on a scale from 1 (early) to 0 (late).

MOL #68767

Results

An unliganded *Torpedo* AChR transmitter binding site is shown in Figs. 1A and 1B (Unwin, 2005). The model we used for quantifying AChR function is a cyclic activation scheme (Fig. 1C). In this scheme the resting R state has a low affinity for ACh and a closed channel, and the active R* state has a high affinity for ACh and an open channel. The R and R* shapes must be different insofar as they have different functional properties.

The cyclic scheme predicts that AChRs should open and close spontaneously, in the absence of exogenous agonists (the R \leftrightarrow R* step). Such events are indeed present in wt AChRs. Jackson (Jackson, 1986) estimated that in embryonic mouse muscle the unliganded gating equilibrium constant $E_0 \sim 10^{-7}$. In adult mouse muscle AChRs expressed in HEK cells, $E_0 \sim 6.5 \times 10^{-7}$ (Jha and Auerbach, 2010; Purohit and Auerbach, 2009). In AChRs the allosteric constant E_0 is small, but it is measurably different from zero. Mutations that increase E_0 in human AChRs are the fundamental cause of some congenital myasthenic syndromes (Zhou et al., 1999).

The adult mouse AChR binding sites have approximately equal affinities for ACh (Jha and Auerbach, 2010; Salamone et al., 1999), so there are only four equilibrium constants to consider in the cyclic scheme: the dissociation constant of the R conformation (K_d), the dissociation constant of the R* conformation (J_d), the diliganded gating constant (E_2) and the allosteric constant (E_0). Without an external energy source the energy required to move from R to A₂R* must be the same for the clockwise and counterclockwise paths, hence,

$$E_2 = E_0 \lambda^2 \quad \text{Eq. 1}$$

MOL #68767

where $\lambda = K_d/J_d$. The efficacy of an agonist (which is a function only of E_2) is the product of two more-fundamental parameters: the allosteric constant (E_0) and the coupling constant (λ) at two transmitter binding sites. In our wt preparation, $\lambda^{ACh} \approx 6600$.

Our objective was to measure E_2 and E_0 for different loop B mutations and calculate λ [$=\sqrt{(E_2/E_0)}$]. For each mutation, the energy (kcal/mol) from the ligand affinity change is $\Delta G^{bind} = -0.59 \ln(\lambda)$ and the energy change for unliganded gating is $\Delta \Delta G^{gate} = -0.59 \ln(E_0^{mut}/E_0^{wt})$. In wt AChRs, we estimate that each ACh molecule is $\Delta G^{bind} \approx -5.2$ kcal/mol more stably bound in R^* vs. R . We also calculated the change in binding energy caused by the mutation, $\Delta \Delta G^{bind} = \Delta G^{bind, mut} - \Delta G^{bind, wt}$.

α G147

The results for α G147 are summarized in Fig. 2A. This residue is conserved in mouse AChR α -subunits and is also present in the acetylcholine binding protein. We examined 10 different side chain substitutions of this amino acid (A, S, V, D, E, R, K, W, Y and P), but single-channel currents activated by 1 mM ACh were apparent only with the S, A and V mutants. Some of the silent α G147 mutations express functional AChRs (see below). The α G147S, A and V single-channel currents were apparent but did not occur in clusters when activated by 1 mM ACh. The effective opening rate at this concentration ($R \rightarrow A_2R^*$) is small either because K_d was large, E_2 was small or both.

In order to enhance cluster formation and allow the estimation of gating rate and equilibrium constants we expressed these mutants on a background that increased E_2 by ~ 450 -fold (see Fig. S1 for example current traces). This background ‘boosts’ E_0 to allow cluster formation and rate constant estimation but has no effect on the loop B mutation’s

MOL #68767

effects on E_0 or λ . Using this background, and by fully-saturating the transmitter binding sites by using 140 mM ACh (Fig. S2), we estimate that the α G147S, A and V mutations indeed decrease E_2^{ACh} substantially (Table S1).

Our next objective was to measure E_0 for the α G147 mutants. For these experiments, we used a background construct that was active spontaneously so that the effect of the loop B mutation could be estimated directly from the durations of intervals within spontaneous clusters (Purohit and Auerbach, 2009). With this background, 6 of the 10 substitutions at α G147 (A, S, V, E, K, Y) produced spontaneous single-channel current clusters. D, R, P and W side chain substitutions did not result in the expression of functional AChRs. All of the expressing mutants reduced E_0 relative to the background (Table S2). However, even the largest reduction (α G147V) was modest, only ~20-fold less than the background.

With these estimates of E_0 and E_2 for the Ser, Ala and Val mutants of α G147 we calculated λ and ΔG^{bind} for ACh (Table S3). On average, for these three α G147 mutants $\lambda^{\text{ACh}} \sim 194$ and $\Delta \Delta G^{\text{bind}} \sim +2.1$ kcal/mol. Compared to the wt values for ACh, these mutations decreased the net ACh binding energy by ~60 %. In contrast, the average effect of these mutations on the allosteric constant was smaller ($\Delta \Delta G^{\text{gate}} \sim +1.4$ kcal/mol). The main effect of mutating α G147 is to reduce the amount of energy made available by the affinity change at the transmitter binding site.

The slope of the R/E plot (Φ) for the α G147 diliganded gating was 0.86 (Fig. 2A). This indicates that with ACh present in the binding sites, this residue experiences a change in energy near the onset of the channel-opening process, about at the same time as the energy change of the agonist molecule itself (Grosman et al., 2000). Interestingly, the

MOL #68767

Φ -value for the unliganded reaction (0.76), although high, was smaller than that for the diliganded reaction.

The reduction in λ^{ACh} in αG147S could be caused by an increase in the R affinity (a decrease in K_d), a decrease in the R* affinity (an increase in J_d) or both. We estimated K_d by examining the αG147S mutant activated by different concentrations of ACh (Fig. 3A). We estimate that K_d for ACh in this construct is ~ 3.6 mM, which is ~ 25 times higher than the wt (Chakrapani et al., 2003). Using the E_2 and E_0 values for this mutant and Eq. 1, we calculate J_d for ACh in this construct is 12.1 μM , which is ~ 550 times higher than the wt (Jha and Auerbach, 2010). Thus, the reduction in the amount of energy made available by the affinity change at the transmitter binding site can be attributed mainly to a decreased affinity for ACh in the R* conformation of the binding site.

αW149

αW149 is an important binding site residue that provides binding energy to the ligand in both the R and R* conformations, probably by cation- π interactions (Zhong et al., 1998). Previously, we showed that mutations of αW149 also influence E_0 (Purohit and Auerbach, 2010). Some of these mutations caused a substantial increase in E_0 ($\Delta\Delta G^{\text{gate}} = -2.3$ kcal/mol for αW149C), but most had more modest or negligible effects ($\Delta\Delta G^{\text{gate}} = +0.3$ kcal/mol for αW149M).

We measured the effects of αW149 mutations on diliganded gating in order to estimate λ^{ACh} (Fig. 2B and Fig. 1S). All of the tested mutations reduced E_2 , with the largest effect being a $\sim 10,000$ -fold reduction for αW149M (Table S1). For all mutants, the predominant effect was to reduce the net agonist binding energy. The clearest

MOL #68767

example is α W149M, for which E_0 was almost unchanged but λ^{ACh} decreased by ~80-fold ($\Delta\Delta G^{\text{bind}} = +2.6$ kcal/mol). On average, the α W149 mutations reduced the R vs. R* ACh binding energy by ~50%.

As was the case with α G147, the diliganded Φ value for α W149 was higher than the corresponding value for unliganded gating (0.94 vs. 0.82) (Fig. 2B).

α G153

α G153 is an interesting loop B residue because a Ser here reduces K_d and causes a myasthenic syndrome (Sine et al., 1995). Also, AChRs that have a high affinity for nicotine (with $\alpha 2$, $\alpha 3$ or $\alpha 4$ subunits) have Lys here while those that do not ($\alpha 1$ or $\alpha 7$) have a Gly. We measured E_0 and E_2 for several α G153 mutants. In these experiments we used the partial agonist choline (Cho) because α G153 mutations increased the opening rate constant to such an extent that it was not possible to obtain estimates using ACh.

All of the tested α G153 side-chain substitutions (K, W, D, C, R, Y, A, P and S) produced functional AChRs that had a higher E_2 values compared to wt (Fig. 2C and Table S1). We also measured E_0 for all 9 of these α G153 mutants. AChRs with W, D, R or Y substitutions produced single-channel currents having multiple open/closed components (see below). The fractional contribution of each of these components was variable between patches, to an extent that E_0 could not be estimated reliably. The other substitutions had more simple kinetic behavior and exhibited clearly-predominant open and closed components. All of these substitutions increased E_0 relative to the background, from 206-fold for Lys to 28-fold for Ser (Table S2).

MOL #68767

The fold-changes in E_2 vs. E_0 for the α G153 mutations are shown in Fig. S3. The maximum effect on both E_2 and E_0 was for the Lys substitution. Overall, the fold-changes in E_2 and E_0 were linearly correlated ($r^2=0.99$) (Fig. S3). This result indicates that α G153 mutations alter diliganded gating by an approximately parallel change E_0 and have almost no effect on λ^{Cho} (Table S3). Indeed, the average $\Delta\Delta G^{\text{bind}}$ for the K, C A, P and S mutants was only +0.3 kcal/mol. Although α G153 mutations increase the affinity of the resting binding site, they have the same quantitative effect on the affinity of the active binding site. We conclude that α G153 makes essentially no contribution to the binding energy difference between R and R*.

As was the case for α G147 and α W149, the α G153 diliganded Φ -value was higher than that for unliganded gating (0.96 vs. 0.79) (Fig. 2C).

We also measured the single-site association and dissociation rate constants and equilibrium dissociation constant for Cho binding to the resting conformation, for four different α G153 mutants (S, A, D and K) (Fig. 3B and Table S4). All of the mutations reduced K_d (increased the resting affinity) compared to the wt (Table S4), to approximately the same extent (mean, ~14-fold).

Other loop B mutations

We measured E_2 and E_0 for Ala side-chain substitutions at the five residues between the two loop B glycines (T148, W149, T150, Y151 and D152). All of these constructs except α W149A resulted in only small (<2-fold) changes in both E_2 and E_0 compared to the wt (Tables S1 and S2 and Fig. S1F). In α W149A, E_0 increased by ~8-fold, but E_2

MOL #68767

decreased by ~134-fold. Using Eq. 1 we estimate that for this mutant $\lambda^{\text{ACh}} \sim 200$ and $\Delta\Delta G^{\text{bind}} = +2.0$ kcal/mol.

The E_0 values were estimated for a few additional mutants of these positions (Table S2 and Fig. S1). At residue αD152 , only the Ala substitution resulted in functional AChRs (no currents for W, K, R or Y). At positions αT148 , αT150 and αY151 , the largest fold-decrease in E_0 was for αT150Y (~25-fold).

Global estimates for the energetic consequences of loop B perturbations from R/E plots for all the mutants are shown in Fig. S4. The Φ -values for diliganded and unliganded gating were 0.92 and 0.77, respectively. The largest fold-increase in E_0 was for αG153K and the largest fold-decrease was for αT150Y . This range (for both α -subunits combined) corresponds to an energy of ~5.5 kcal/mol.

Multiple open-channel lifetimes

We now turn to the description of multiple open-time components, which are common in unliganded AChRs (Grosman, 2003; Jackson, 1986; Mukhtasimova et al., 2009; Purohit and Auerbach, 2009). These events are worth examining, in part, because they have been interpreted as reflecting an intermediate state in the channel-opening conformational cascade (Mukhtasimova et al., 2009). Previously we reported that many binding site mutations eliminate this long-lived component [αY93 (loop A), αW149 (loop B), and $\alpha\text{Y190}/\alpha\text{Y198}$ (loop C)], even when combined with distant mutations in the transmembrane domain that alone make it more prevalent simply because these have low Φ values and therefore slow all closures (Purohit and Auerbach, 2010). This

MOL #68767

observation led us to conclude that the long openings arise from local structural fluctuations of binding site residues, primarily of α W149.

α G153 mutations did not eliminate the long-open component, and in fact and enhanced them in some cases. We therefore tested whether or not substitutions at the abovementioned positions that eliminate spontaneous long openings do so when a α G153S mutation is also present (Fig. 4). We examined five double-mutant pairs, α G153S+[α W149F, α Y93F, α Y190F, α Y198F or α G147S] where the bracketed mutation was previously shown to eliminate long openings. The α W149F, α Y198F and α G147S mutations again eliminated the long open component but the α Y93F and α Y190F substitutions no longer did.

Inter-residue coupling energies for α G153S paired with a Phe substitution at four α subunit binding site aromatic residues (α Y93, α W149, α Y190 and α Y198) and α G147 are shown in Table S5. In all cases the Ser-Phe side chain pairs behaved nearly independently in unliganded gating.

MOL #68767

Discussion

The results (summarized in Fig. 5 and Table 1) provide insight into the nature of the energy changes at the AChR transmitter binding site when it changes conformation between its low-affinity R and high-affinity R* conformation. It is this change in conformation that triggers the gating conformational cascade and determines ligand efficacy.

In brief, α G147 and α G153 appear to act as hinges that influence the allosteric constant (E_0), the resting affinity (K_d) and the agonist affinity ratio (λ). However, these hinges have opposite actions. Mutations of α G147 change the above parameters so that there is a decrease in the channel-open probability (P_o), whereas α G153 mutations change them to cause an increase in P_o . Below, we associate a change in energy with a local change in structure (a ‘strain’ or ‘movement’ of the perturbed position relative to its immediate environment), and use the word ‘favorable’ to describe a molecular motion that increases P_o .

α G147 mutations reduced E_0 , which is to say that in the absence of agonists the energy change associated with the gating motion of this residue is unfavorable for all side chain substitutions. Although we cannot with certainty identify the structural correlate(s) of this unfavorable energy change, there are some clues. Because all tested side chains substitutions were unfavorable, we speculate that in the absence of ligands there is a favorable gating motion in the wt that requires flexibility of the backbone (an ‘activation’ hinge). However, different amino acid substitutions caused modestly different degrees of energy change, so side chain interactions, too, are also likely to be involved. Because the

MOL #68767

larger Val side chain experienced the largest gating energy change, it is possible that steric hindrance is a factor that sets the magnitude of E_0 .

Using the cyclic activation scheme and Eq. 1 (see below) we conclude that the α G147S, A and V mutants reduce λ^{ACh} from ~6600 in the wt to ~194. This corresponds to a net loss in ACh binding energy of $\Delta\Delta G^{\text{bind}} \sim +2.1$ kcal/mol/site. The α G147S mutation reduced the affinity of both the resting and active binding sites, but the effect was larger for R^* compared to R. Hence, the main effect of this mutation appears to be to reduce the stability of the bound transmitter in the R^* conformation. This implies that with ligand present in wt AChRs, at the onset of the forward isomerization the structural change at α G147 results in a net favorable energetic interaction of the protein with the transmitter molecule.

There are some hints regarding the structural basis of this event. Ser and Ala are both small and have a similar effect on λ^{ACh} whereas the larger Val side chain had a somewhat larger effect. This suggests that $\Delta\Delta G^{\text{bind}}$ is influenced by side chain size as well as by the elimination of the abovementioned intrinsic favorable backbone motion. α G147 is far from the ligand (Celie et al., 2004), so this binding energy change is likely to be indirect and involve additional structural elements at the binding site. Regardless, without the activation hinge at position α G147 the residual net ACh binding energy is reduced from -5.2 to -3.1 kcal/mol/site. Interfering with the gating motion of α G147 decreases the binding energy used to promote gating by ~60%.

Mutations of α W149 had approximately the same magnitude of effect on E_0 as those at position α G147, but in contrast without agonists most α W149 side chains substitutions were *more* stable in R^* compared to R. The order of effect

MOL #68767

(C>T>A>V>N>M) does not immediately suggest a chemical basis of the more-favorable R* environment around α W149 in the unliganded site, except to note that the energy changes varied substantially with different side chains and that steric hindrance does not appear to be a factor. We speculate that the gating motion of α W149 in the unliganded binding site involves a change in the positions of side chain atoms in a spatially-unrestricted environment.

The α W149 mutant binding energy changes were large and unfavorable for all substitutions. There was only a small range of energies for the binding energy loss (\sim 0.6 kcal/mol, Ala to Asn), which suggests that for the residues we examined only Trp provides the extra stabilization energy to the bound ligand, probably *via* a cation- π interaction (Zhong et al., 1998). This energy constitutes about half of the total net ACh binding energy change. We speculate that the residual binding energy (\sim 2.7 kcal/mol/site) comes from interactions between the ligand and other binding site entities, in particular, α Y190 (Purohit and Auerbach, 2010).

α G153 is quite different from both α G147 and α W149. Essentially all of the energetic effects of mutations here were with regard to E_0 , with very little with regard to λ^{Cho} . In the unliganded binding site, α G153 moves and, as was the case with α W149, with side chains substitutions here the AChR was in all case *more* stable in R* compared to R. The fact that the E_0 range of gating energy change here was small (\sim 1 kcal/mol) suggests that side chain size does not play a significant role. We speculate that both in the presence and absence of agonists this glycine adopts an unfavorable R* backbone configuration (a ‘deactivation’ hinge) and that all mutations here prevent this from happening.

MOL #68767

Although all α G153 mutations reduced K_d (see below) they also reduced J_d to approximately the same extent (Table S4). We conclude that the α G153 does not provide agonist binding energy for the gating isomerization, either directly or indirectly. This conclusion bears directly on the recent report proposing that the α G153 side chain is the basis for differences in the EC_{50} value for the partial agonist nicotine in different AChRs (Xiu et al., 2009). The observations that led to this hypothesis were that the α G153K mutation decreases the neuromuscular EC_{50} for nicotine and restores the fingerprint of a cation- π interaction between α W149 and this agonist. EC_{50} is a complex parameter that reflects both binding and gating. Our results suggest that for α G153K, the 14-fold reduction in EC_{50} can be attributed almost completely to the 206-fold increase in E_0 . Our evidence suggests that a Lys side chain at this position increases the efficacy of all agonists equally and not specifically that of nicotine.

Previously we reported that for seven different locations (all far from the binding sites), Φ values were the same for diliganded and unliganded gating (Purohit and Auerbach, 2009). Here, we found that the Φ values for α G147, α W149 and α G153 were all higher in the liganded vs. unliganded condition. This implies that these residues experience their gating energy change relatively earlier when an agonist molecule is nearby. This could be because the residue itself moves earlier, the peak transition state for the overall protein isomerization occurs later, or both. Regardless, the shift in Φ is an indication of an ‘induced fit’, whereby the agonist molecule perturbs (rearranges) the binding site so as to alter the timing, pathway or ground states of the isomerization. The effect we have observed is small and other results suggest that the cyclic scheme is still a valid approximation even with a perturbed binding site, namely that many different

MOL #68767

agonists have the same Φ value (Grosman et al., 2000) and that the effect of α G153 mutations can be explained simply by a change in E_0 . Nonetheless, the shift in Φ values with vs. without ligand suggests that the cyclic scheme and Eq. 1 may not pertain in detail to all AChRs that have binding site perturbations.

An ancillary part of this study was to measure K_d and calculate J_d for a few mutant constructs of the two loop B Gly residues. These equilibrium constants pertain to ligand binding and the underlying molecular movements for this separate process may or may not be distinct from those for gating. Mutations of α G147 and α G153 had opposite effects on K_d . The α G147S mutation reduced the affinity of the resting binding site for ACh while four different substitutions of α G153 increased this affinity. Apparently, backbone flexibility at these positions, perhaps in combination, is important for allowing agonists to bind with the physiologically-appropriate resting affinity.

The long openings in spontaneous currents appear to arise from a local isomerization of the α W149 side chain (Purohit and Auerbach, 2010). This fluctuation in structure is delicate because it can be eliminated by a variety of binding site perturbations, including the presence of an agonist molecule, all α W149 side chain substitutions, and most substitutions of α G147, α Y93, α Y190 and α Y198 (but not of α G153 and ϵ/δ W55/57). We speculate that in the absence of a ligand there is a network of interactions, local to the binding site that permits α W149 to adopt alternative conformations. One of these is associated with the relatively-rare, long openings.

In summary, loop B has two glycine hinges that have opposing actions in binding and gating of wt AChRs. Removal of the ‘activation’ hinge at α G147 decreases P_o by reducing K_d , E_0 and λ . The main effect of interfering with this hinge is to reduce the

MOL #68767

affinity of the active conformation of the binding site and, hence, the amount of binding energy available to promote gating. Also, mutation α G147 eliminates long openings that likely arise from alternative conformations of α W149. The ‘deactivation’ hinge at α G153 plays an inverse role. Interfering with the operation of this hinge increases P_o by increasing both K_d and E_0 but has essentially no consequence with regard to λ . Mutations of α G153 also increase the probability of long openings. Between these two hinges is α W149, a residue that provides about half of the binding energy towards the gating isomerization. It is possible that the two opposing glycine hinges act in concert (along with other elements at the binding site) to determine E_0 and K_d and to position the central tryptophan so that it provides the physiologically-appropriate binding energy to generate the synaptic response.

MOL #68767

Acknowledgements

We thank M. Shero, M. Merritt and M. Teeling for technical assistance.

MOL #68767

Authorship Contributions

PP designed, conducted and analyzed all the experiments and assisted AA in writing the paper.

MOL #68767

References

- Abramson SN, Li Y, Culver P and Taylor P (1989) An analog of lophotoxin reacts covalently with Tyr190 in the alpha-subunit of the nicotinic acetylcholine receptor, pp 12666-12672.
- Akk G (2001) Aromatics at the murine nicotinic receptor agonist binding site: mutational analysis of the alphaY93 and alphaW149 residues. *J Physiol* **535**(Pt 3):729-740.
- Akk G, Sine S and Auerbach A (1996) Binding sites contribute unequally to the gating of mouse nicotinic α D200N acetylcholine receptors. *J Physiol* **496** (Pt 1):185-196.
- Auerbach A (2010) The gating isomerization of neuromuscular acetylcholine receptors. *The Journal of Physiology* **588**(4):573-586.
- Auerbach A, Sigurdson W, Chen J and Akk G (1996) Voltage dependence of mouse acetylcholine receptor gating: different charge movements in di-, mono- and unliganded receptors. *J Physiol* **494** (Pt 1):155-170.
- Aylwin ML and White MM (1994) Ligand-receptor interactions in the nicotinic acetylcholine receptor probed using multiple substitutions at conserved tyrosines on the alpha subunit. *FEBS Lett* **349**(1):99-103.
- Cashin AL, Torrice MM, McMenimen KA, Lester HA and Dougherty DA (2007) Chemical-scale studies on the role of a conserved aspartate in preorganizing the agonist binding site of the nicotinic acetylcholine receptor. *Biochemistry* **46**(3):630-639.
- Celie PH, van Rossum-Fikkert SE, van Dijk WJ, Brejc K, Smit AB and Sixma TK (2004) Nicotine and carbamylcholine binding to nicotinic acetylcholine receptors as studied in AChBP crystal structures. *Neuron* **41**(6):907-914.
- Chakrapani S, Bailey TD and Auerbach A (2003) The role of Loop 5 in acetylcholine receptor channel gating. *J Gen Physiol* **122**(5):521-539.
- Chen J, Zhang Y, Akk G, Sine S and Auerbach A (1995) Activation kinetics of recombinant mouse nicotinic acetylcholine receptors: mutations of alpha-subunit tyrosine 190 affect both binding and gating. *Biophys J* **69**(3):849-859.
- Chiara DC, Middleton RE and Cohen JB (1998) Identification of tryptophan 55 as the primary site of [3H]nicotine photoincorporation in the gamma-subunit of the Torpedo nicotinic acetylcholine receptor. *FEBS Lett* **423**(2):223-226.
- Cohen JB, Sharp SD and Liu WS (1991) Structure of the agonist-binding site of the nicotinic acetylcholine receptor. [3H]acetylcholine mustard identifies residues in the cation-binding subsite, pp 23354-23364.
- Dennis M, Giraudat J, Kotzyba-Hibert F, Goeldner M, Hirth C, Chang JY, Lazure C, Chretien M and Changeux JP (1988) Amino acids of the Torpedo marmorata acetylcholine receptor .alpha. subunit labeled by a photoaffinity ligand for the acetylcholine binding site. *Biochemistry* **27**(7):2346-2357.
- Edelstein S and Changeux J-P (1998) Allosteric transitions of the acetylcholine receptor. *Adv Protein Chem* **51**:121-184.
- Fersht AR (1995) Characterizing transition states in protein folding: an essential step in the puzzle. *Curr Opin Struct Biol* **5**(1):79-84.
- Galzi JL, Revah F, Black D, Goeldner M, Hirth C and Changeux JP (1990) Identification of a novel amino acid alpha-tyrosine 93 within the cholinergic ligands-binding

MOL #68767

- sites of the acetylcholine receptor by photoaffinity labeling. Additional evidence for a three-loop model of the cholinergic ligands-binding sites, pp 10430-10437.
- Grosman C (2003) Free-Energy Landscapes of Ion-Channel Gating Are Malleable: Changes in the Number of Bound Ligands Are Accompanied by Changes in the Location of the Transition State in Acetylcholine-Receptor Channels. *Biochemistry* **42**(50):14977-14987.
- Grosman C, Zhou M and Auerbach A (2000) Mapping the conformational wave of acetylcholine receptor channel gating. *Nature* **403**(6771):773.
- Jackson MB (1986) Kinetics of unliganded acetylcholine receptor channel gating. *Biophys J* **49**(3):663-672.
- Jha A and Auerbach A (2010) Acetylcholine receptor channels activated by a single agonist molecule. *Biophys J* **98**(9):1840-1846.
- Jha A, Purohit P and Auerbach A (2009) Energy and structure of the M2 helix in acetylcholine receptor-channel gating. *Biophys J* **96**(10):4075-4084.
- Karlin A (2002) Emerging structure of the nicotinic acetylcholine receptors. *Nature Rev Neurosci* **3**:102.
- Lee WY and Sine SM (2004) Invariant aspartic Acid in muscle nicotinic receptor contributes selectively to the kinetics of agonist binding. *J Gen Physiol* **124**(5):555-567.
- Liu Z, Williamson MS, Lansdell SJ, Denholm I, Han Z and Millar NS (2005) A nicotinic acetylcholine receptor mutation conferring target-site resistance to imidacloprid in *Nilaparvata lugens* (brown planthopper). *Proc Natl Acad Sci U S A* **102**(24):8420-8425.
- Middleton RE and Cohen JB (1991) Mapping of the acetylcholine binding site of the nicotinic acetylcholine receptor: [3H]nicotine as an agonist photoaffinity label. *Biochemistry* **30**(28):6987-6997.
- Mitra A, Cymes GD and Auerbach A (2005) Dynamics of the acetylcholine receptor pore at the gating transition state. *Proc Natl Acad Sci USA* **102**(42):15069-15074.
- Mukhtasimova N, Lee WY, Wang HL and Sine SM (2009) Detection and trapping of intermediate states priming nicotinic receptor channel opening. *Nature* **459**(7245):451-454.
- O'Leary ME, Filatov GN and White MM (1994) Characterization of d-tubocurarine binding site of Torpedo acetylcholine receptor. *Am J Physiol* **266**(3):C648-653.
- Purohit P and Auerbach A (2007) Acetylcholine Receptor Gating: Movement in the α -Subunit Extracellular Domain. *J Gen Physiol* **130**(6):569-579.
- Purohit P and Auerbach A (2009) Unliganded gating of acetylcholine receptor channels. *Proc Natl Acad Sci U S A* **106**(1):115-120.
- Purohit P and Auerbach A (2010) Energetics of gating at the apo-acetylcholine receptor transmitter binding site. *J Gen Physiol* **135**(4):321-331.
- Qin F (2004) Restoration of single-channel currents using the segmental k-means method based on hidden Markov modeling. *Biophys J* **86**:1488.
- Qin F, Auerbach A and Sachs F (1997) Maximum likelihood estimation of aggregated Markov processes. *Proc Biol Sci* **264**(1380):375-383.
- Salamone FN, Zhou M and Auerbach A (1999) A re-examination of adult mouse nicotinic acetylcholine receptor channel activation kinetics. *J Physiol* **516** (Pt 2):315-330.

MOL #68767

- Sine SM, Ohno K, Bouzat C, Auerbach A, Milone M, Pruitt JN and Engel AG (1995) Mutation of the acetylcholine receptor alpha subunit causes a slow-channel myasthenic syndrome by enhancing agonist binding affinity. *Neuron* **15**(1):229-239.
- Sine SM, Quiram P, Papanikolaou F, Kreienkamp HJ and Taylor P (1994) Conserved tyrosines in the alpha subunit of the nicotinic acetylcholine receptor stabilize quaternary ammonium groups of agonists and curariform antagonists. *J Biol Chem* **269**(12):8808-8816.
- Sugiyama N, Boyd AE and Taylor P (1996) Anionic residue in the alpha-subunit of the nicotinic acetylcholine receptor contributing to subunit assembly and ligand binding. *J Biol Chem* **271**(43):26575-26581.
- Unwin N (2005) Refined structure of the nicotinic acetylcholine receptor at 4 Å resolution. *J Mol Biol* **346**(4):967.
- Xiu X, Puskar NL, Shanata JA, Lester HA and Dougherty DA (2009) Nicotine binding to brain receptors requires a strong cation-pi interaction. *Nature* **458**(7237):534-537.
- Zhong W, Gallivan JP, Zhang Y, Li L, Lester HA and Dougherty DA (1998) From ab initio quantum mechanics to molecular neurobiology: a cation- π binding site in the nicotinic receptor. *Proc Natl Acad Sci U S A* **95**(21):12088-12093.
- Zhou M (1999) Molecular recognition at the transmitter binding site of the nicotinic acetylcholine receptor channel, in *The Department Physiology and Biophysics* p 176, SUNY at Buffalo, Buffalo.
- Zhou M, Engel AG and Auerbach A (1999) Serum choline activates mutant acetylcholine receptors that cause slow channel congenital myasthenic syndromes. *PNAS* **96**(18):10466-10471.

MOL #68767

Footnotes

This work was supported by National Institute of Health [NS-064969].

MOL #68767

Figure Legends

Figure 1. AChR structure and function. A. The transmitter binding site. Left, Unliganded *Torpedo* AChR (2bg.pdb9(Unwin, 2005)). Subunits: α_γ , gray and β/δ , light blue (γ and α_δ not displayed). Boxed area is the α_γ transmitter binding site. Horizontal lines approximately mark the membrane. Right, close-up of the α_γ binding site. Green, loop A ($\alpha Y93$ shown); tan, loop C ($\alpha Y190$ shown); magenta, loop B (all side chains 147-153 shown; C α atoms of $\alpha G147$ and $\alpha G153$ as spheres). **B.** Cyclic activation scheme for the AChR. A is the agonist and the other bold letters represent stable ground states (structural ensembles represented by wells in an energy diagram). Paired arrows represent the unstable intermediates that connect the ground states. R, resting (low affinity for the agonist and low ionic conductance); R*, active (high affinity for the agonist and high ionic conductance); D, desensitized states (high affinity for the agonist and low ionic conductance) are gray. Next to the arrows are the salient equilibrium constants. E_0 , unliganded (spontaneous) gating; E_1 monoliganded gating; E_2 diliganded gating; K_d , dissociation constant for agonist binding to R; J_d , dissociation constant for agonist binding to R*. The two binding sites have approximately the same K_d and J_d for ACh and choline (Jha and Auerbach, 2010). Without an external energy source the net energy change, R-to- A_2R^* , must be equal for the ‘physiological’ pathway $R \leftrightarrow AR \leftrightarrow A_2R \leftrightarrow A_2R^*$ (Scheme 1) and for the alternative pathway $R \leftrightarrow R^* \leftrightarrow AR^* \leftrightarrow A_2R^*$. Hence, $E_2/K_d^2 = E_0/J_d^2$, or $E_2 = E_0 \lambda^2$ (Eq. 1).

Figure 2. Rate/equilibrium constant (R/E) relationships for three loop B residues.

Left, diliganded gating and right, unliganded (spontaneous) gating. The x-axis is the

MOL #68767

logarithm of the gating equilibrium constant (E_2 or E_0) and the y-axis is the logarithm of the forward, channel-opening rate constant (f_2 or f_0). **A.** α G147 mutations reduce E_2 more so than E_0 . **B.** α W149 mutations reduce E_2 but mainly increase E_0 (values from (Purohit and Auerbach, 2010)). **C.** α G153 mutations increase E_2 and E_0 to similar extents (See Fig S3). The kinetic parameters are shown in Tables S1 and S2. The number in each panel is the R/E slope (Φ) \pm s.d. of the linear fit, which gives the relative timing of the residue's gating motion (larger is earlier). All three residues move early, but the diliganded Φ values are larger than the unliganded ones.

Figure 3. Equilibrium dissociation constants. **A,** The affinity of the resting α G147S AChR for ACh was estimated from the P_o dose-response profile. **B,** K_d value for choline were estimated for α G153S by fitting interval durations across concentrations. The rate constants and K_d values for all α G153 mutants were similar and are given in Table S4.

Figure 4. Multiple open components. Example histograms and single-channel current traces for different loop B mutants. Arrow indicates the long-opening component. There was no agonist present (spontaneous currents). In all constructs the background was α DYS (see Supplemental Information). Long openings are apparent in the background (no binding site mutations) and with the binding site mutations α G153S, (α G153S+ α Y93F) and (α G153S+ α Y190F). They were absent with the mutations (α G153S+ α G147S) and (α G153S+ α Y198F). The long openings possibly arise from a local isomerization of α W149 (Purohit and Auerbach, 2010).

MOL #68767

Figure 5. Binding site mutations change the energy of intrinsic gating and agonist

binding. Closed symbols, the gating free energy change [$\Delta\Delta G^{\text{gate}} = -0.59\ln(E_0^{\text{mut}}/E_0^{\text{wt}})$], in

kcal/mol]. Open symbols, the binding free energy change or [$\Delta\Delta G^{\text{bind}} = -0.59\ln(\lambda^{\text{mut}}/\lambda^{\text{wt}})$].

Favorable mutations (that produce a negative $\Delta\Delta G$) increase the open probability (P_o).

Left to Right: α G147 mutations are unfavorable with regard to both gating and binding,

but the effect is larger for binding. α W149 mutations mostly are favorable with regard to

gating but have larger and unfavorable effects on binding. α G153 mutations have a large

and favorable effect on gating but little effect on binding. The values are listed in Table 1.

MOL #68767

Table

Table 1: Energy changes of unliganded gating (E_0) and agonist binding (λ) for different loop B mutants.

Construct	Ligand	λ (K_d/J_d ratio)	Net binding $\Delta\Delta G^{\text{bind}}$	Gating $\Delta\Delta G^{\text{gate}}$
wt ^{ACh}	ACh	6587	0.00	0.00
wt ^{cho}	Cho	266	0.00	0.00
G147V	ACh	82	2.59	1.73
A	ACh	215	2.02	1.40
S	ACh	287	1.85	1.12
W149C	ACh	123	2.35	-2.34
T	ACh	161	2.19	-1.43
A	ACh	202	2.06	-1.22
V	ACh	143	2.26	-0.95
N	ACh	69	2.69	-0.63
M	ACh	79	2.61	0.26
G153K	Cho	151	0.34	-3.14
C	Cho	151	0.34	-2.87
P	Cho	159	0.31	-2.49
A	Cho	175	0.25	-2.41
S	Cho	184	0.22	-1.98
T148A	Cho	196	0.18	-0.28
T150A	Cho	161	0.00	-0.64
Y151A	Cho	521	-0.39	1.04
D152A	Cho	339	-0.14	0.13

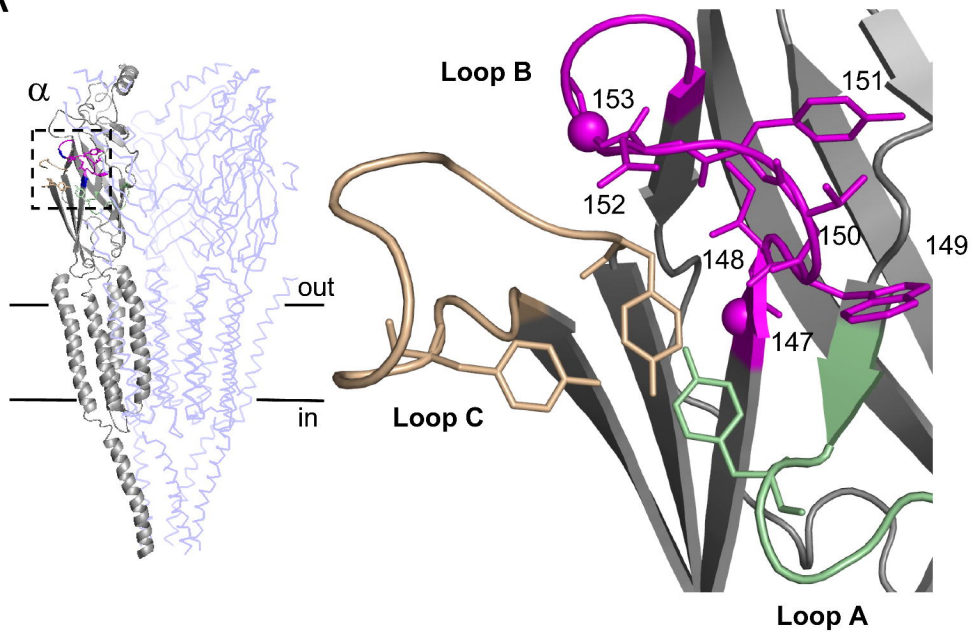
MOL #68767

Table Legend

Table 1. The units are kcal/mol. The values are shown in graphical form for α G147, α W149 and α G153 in Fig. 5. λ is the R/R* affinity ratio (K_d/J_d) for the appropriate agonist. $\Delta\Delta G^{\text{bind}} = -0.59\ln(\lambda^{\text{mut}}/\lambda^{\text{wt}})$ and $\Delta\Delta G^{\text{gate}} = -0.59\ln(E_0^{\text{mut}}/E_0^{\text{wt}})$. See Tables S1-S3.

Figure 1

A



B

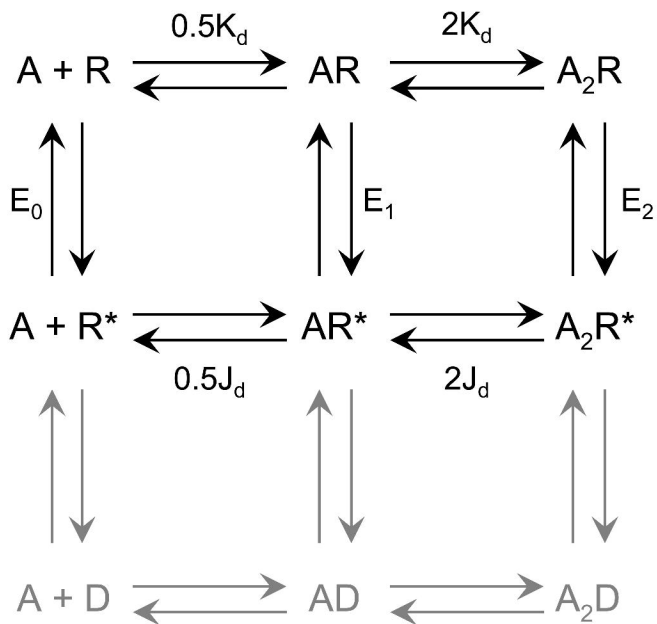
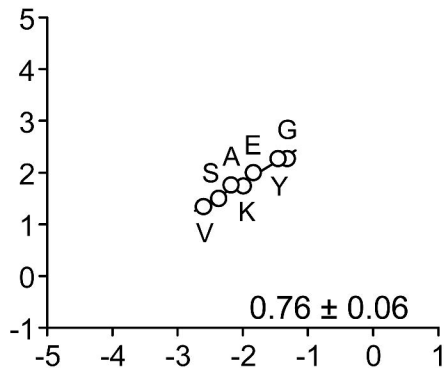
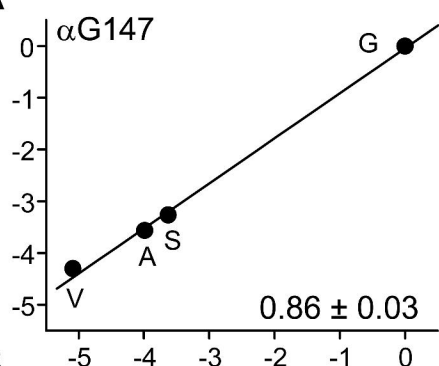
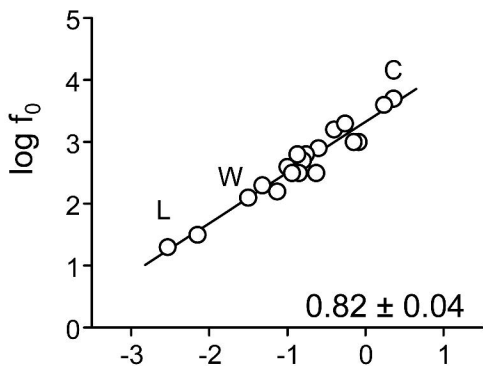
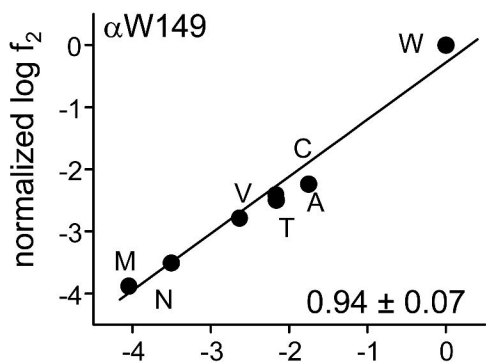


Figure 2

A



B



C

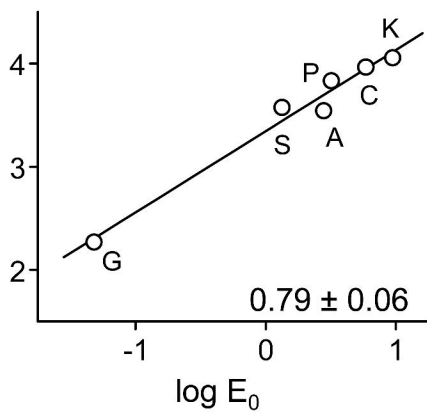
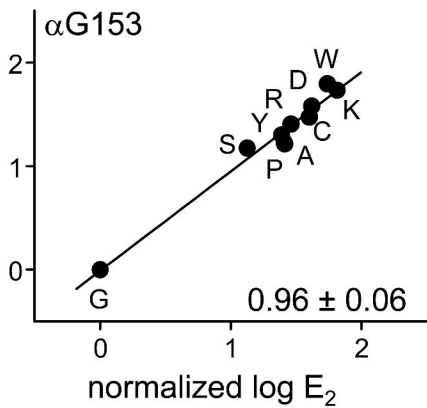
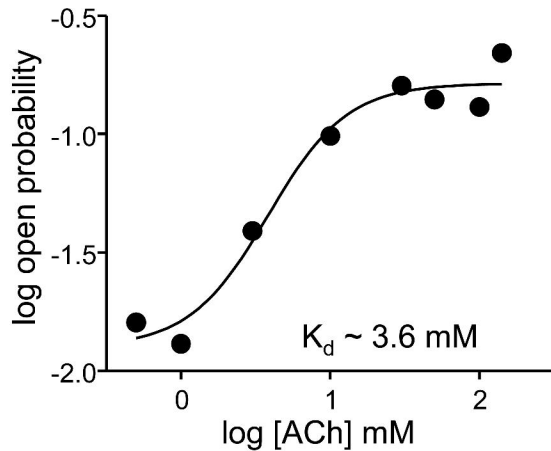
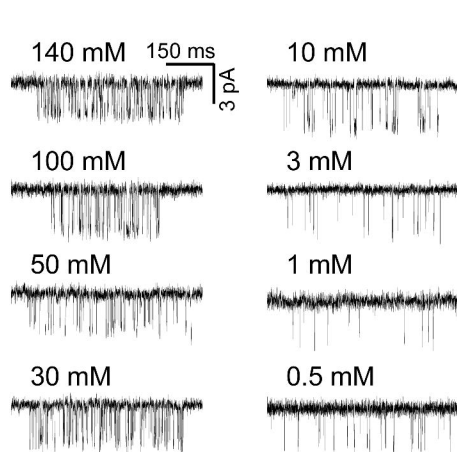


Figure 3

A

α G147S



B

α G153S

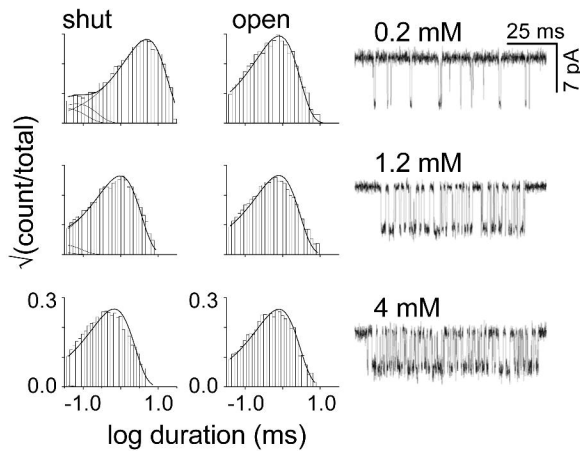


Figure 4

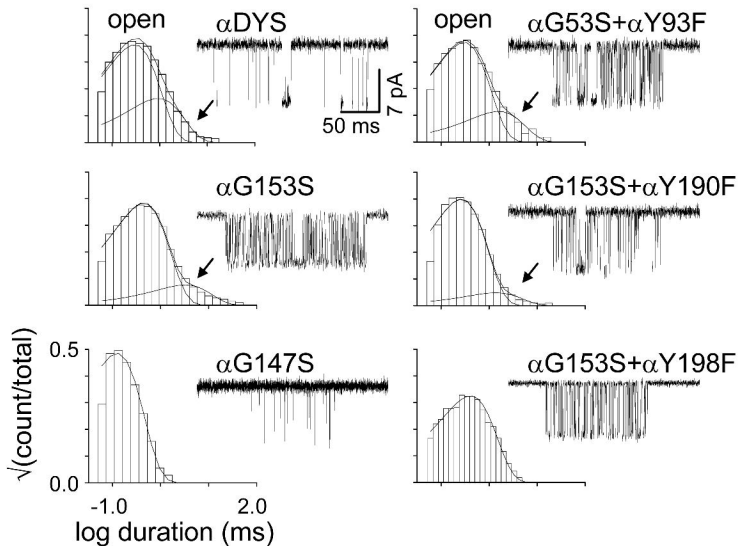


Figure 5

